PHYSICAL REVIEW B **93**, 081409(R) (2016)

Dynamics of nuclear spin polarization induced and detected by coherently precessing electron spins in fluorine-doped ZnSe

F. Heisterkamp,[1] E. Kirstein,[1] A. Greilich,[1] E. A. Zhukov,[1] T. Kazimierczuk,[1,*] D. R. Yakovlev,[1,2] A. Pawlis,[3] and M. Bayer[1,2]

[1]*Experimentelle Physik 2, Technische Universität Dortmund, 44221 Dortmund, Germany*

[2]*Ioffe Institute, Russian Academy of Sciences, 194021 St. Petersburg, Russia*

[3]*Peter Grünberg Institute (PGI-9), Forschungszentrum Jülich, 52425 Jülich, Germany*

(Received 11 January 2016; published 18 February 2016)

We study the dynamics of optically induced nuclear spin polarization in a fluorine-doped ZnSe epilayer via time-resolved Kerr rotation. The nuclear polarization in the vicinity of a fluorine donor is induced by interaction with coherently precessing electron spins in a magnetic field applied in the Voigt geometry. It is detected by nuclei-induced changes in the electron spin coherence signal. This all-optical technique allows us to measure the longitudinal spin relaxation time T_1 of the ^{77}Se isotope in a magnetic field range from 10 to 130 mT under illumination. We combine the optical technique with radio frequency methods to address the coherent spin dynamics of the nuclei and measure Rabi oscillations, Ramsey fringes, and the nuclear spin echo. The inhomogeneous spin dephasing time T_2^* and the spin coherence time T_2 of the ^{77}Se isotope are measured. While the T_1 time is on the order of several milliseconds, the T_2 time is several hundred microseconds. The experimentally determined condition $T_1 \gg T_2$ verifies the validity of the classical model of nuclear spin cooling for describing the optically induced nuclear spin polarization.

DOI: 10.1103/PhysRevB.93.081409

The spin of a donor-bound electron in fluorine-doped ZnSe represents a promising system for quantum information technologies. So far, emission of indistinguishable single photons [1], photon entanglement [2], and optical control of single electron spins [3–5] were achieved. Studies of the electron spin dynamics of an ensemble of donor-bound electrons demonstrated a spin dephasing time T_2^* of 33 ns and a longitudinal spin relaxation time T_1 of 1.6 μs [6,7]. At low temperatures the hyperfine interaction with nuclear spins is the main mechanism limiting the electron spin coherence. ZnSe is a particularly attractive material due to the low natural abundance of isotopes with nonzero nuclear spins [4.11% ^{67}Zn ($I = 5/2$) and 7.58% ^{77}Se ($I = 1/2$)] and the possibility to purify it isotopically such that it does not contain nonzero nuclear spins. However, this approach is technologically demanding. Alternatively, one may search for effects where the polarization of nuclear spins provides favorable conditions for a long-lived electron spin coherence. For example, the nuclear frequency focusing effect of the electron spin coherence in singly charged (In,Ga)As/GaAs quantum dots reduces the electron spin dephasing by driving the precessing ensemble towards a single mode collective motion [8]. In order to understand the underlying mechanisms comprehensive information on the polarization and relaxation dynamics of the nuclei interacting with the electrons driven by periodic laser excitation is required.

We recently demonstrated a spatially inhomogeneous nuclear spin polarization induced in the vicinity of the fluorine donor in a picosecond pump-probe Kerr rotation (KR) experiment on a fluorine-doped ZnSe epilayer [9]. The nuclear spin polarization occurs under excitation with a helicity modulated pump beam, for which the induced average electron spin polarization is expected to be zero. The classical model of nuclear spin cooling was used to explain the induced nuclear spin polarization [10]. It implies that the nuclear spin system can be described using the spin temperature approach, which requires that the longitudinal spin relaxation time T_1 is much longer than the spin coherence time T_2 ($T_1 \gg T_2$). To validate this condition these times need to be measured under the conditions of the pump-probe experiment.

The feasibility of such measurements has been demonstrated in Refs. [11,12] on GaAs/(Al,Ga)As quantum wells (QWs) under optical excitation with a constant circular polarization. Similar to these studies we combine the time-resolved Kerr rotation (TRKR) measurements with radio frequency (rf) techniques to study the coherent spin dynamics of the nuclei, but we perform our studies under helicity modulated excitation. Furthermore, we present an all-optical technique (see also Ref. [13]) employing TRKR in the resonant spin amplification (RSA) regime [14] to also measure the T_1 time. We use these two methods to perform a complete study of the dynamics of the ^{77}Se isotope, whose polarization was studied in Ref. [9], under the conditions of the TRKR experiment and measure the nuclear spin relaxation time T_1, the inhomogeneous spin dephasing time T_2^*, and the spin coherence time T_2. From the results we conclude that the spin temperature approach is valid under these experimental conditions.

We employ a pump-probe scheme to measure TRKR using a mode-locked Ti:sapphire laser with a pulse duration of 1.5 ps at a repetition rate of 75.75 MHz. The circularly polarized pump beam excites the sample along the growth axis and the KR of the linearly polarized probe beam is measured with a balanced photoreceiver connected to a lock-in amplifier. The pump beam is helicity modulated by an electro-optical modulator with the frequency f_m varied from 50 up to 1050 kHz. We conduct all measurements at a fixed small negative time delay of the probe pulses with respect to the pump pulses and scan the magnetic field, i.e., use the RSA regime [14,15]. The probe

*Present address: Institute of Experimental Physics, Faculty of Physics, University of Warsaw, 02-093 Warsaw, Poland.

beam is kept unmodulated. Both beams have a diameter of about 300 μm on the sample. The pump power is kept constant at 8 mW and the probe power at 0.5 mW for all measurements.

We measure the nuclear spin polarization by its influence on the Larmor precession frequency of the donor-bound electron spins in a fluorine-doped ZnSe epilayer with a dopant concentration of about 10^{18} cm^{-3}. The sample was grown by molecular-beam epitaxy on (001)-oriented GaAs substrate. For details about the optical properties and electron spin coherence in this sample we refer to Ref. [6] (sample C). We use a degenerate pump-probe scheme and resonantly excite the donor-bound heavy hole exciton (D^0X-HH) at 2.800 eV. To obtain the required photon energy the laser photon energy is doubled by a beta barium borate crystal. The sample is placed in a cryostat with a superconducting split coil solenoid with the magnetic field oriented perpendicular to the optical axis and the structure growth axis. The sample temperature is fixed at about 1.8 K.

A rf coil near the sample surface allows us to apply in addition rf fields with variable frequency from 50 to 500 kHz. The axis of the coil is oriented along the optical axis. Thus, the oscillating magnetic field is oriented along the optical axis and perpendicular to the external magnetic field. A delay generator allows us to apply well-defined and exactly timed sequences of rf pulses to perform experiments on the nuclear spin coherence.

For the T_1 measurements we use a TTL multiplexer (average propagation delay: 12 ns) in combination with two arbitrary function generators to quickly switch f_m (with a rise time of 8 ns). The signal is continuously demodulated by two lock-in amplifiers, each locked permanently on one of the two modulation frequencies. Their signals are recorded by a fast digitizer card. The time resolution of this setup is given by the digitizer card and the lock-in amplifier, which is the limiting factor here and demodulates the signal at a time constant of 50 μs.

The nuclear spin relaxation time T_1 is measured using an all-optical approach based on fast switching between two different modulation frequencies $f_{m,1}$ and $f_{m,2}$. The first modulation frequency $f_{m,1}$ is close to the optically induced nuclear magnetic resonance (NMR) at the particular magnetic field, while the second one is set to $f_{m,2} = 1050$ kHz, where the NMR can be reached only at a stronger magnetic field.

Figure 1(a) shows two RSA spectra measured at modulation frequencies of $f_{m,1} = 100$ kHz (black line) and $f_{m,2} = 1050$ kHz (green line), respectively. The magnetic field is varied and this, in turn, leads to a change of the electron spin Larmor precession frequency, so that the spins precess either in phase or out of phase with the laser repetition frequency and the RSA signal exhibits characteristic periodic peaks in dependence on the magnetic field perpendicular to the optical axis (Voigt geometry) [15]. Due to optically induced, inhomogeneous nuclear polarization (see Ref. [9] for details) the effective field which determines the electron spin precession depends on the modulation frequency. Thus, the RSA peaks at different modulation frequencies are shifted relative to each other. The red arrow marks the position of the optically induced NMR of the ^{77}Se isotope at $f_{m,1} = 100$ kHz. The black arrow marks the magnetic field position ($B = 15.72$ mT) for the measurement of the T_1 time. Figure 1(b) illustrates the change of the KR signal when the modulation frequency

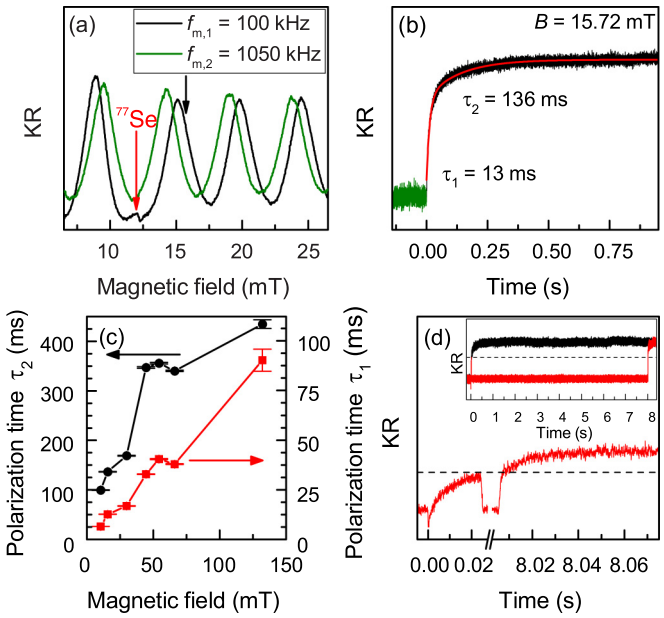

FIG. 1. (a) RSA spectra measured at $f_{m,1} = 100$ kHz (black line) and $f_{m,2} = 1050$ kHz (green line). The red arrow marks the optically induced NMR of the ^{77}Se isotope at $f_{m,1} = 100$ kHz and the black arrow marks the magnetic field position ($B = 15.72$ mT) for the measurement shown in Fig. 1(b). (b) Change of KR amplitude at fixed magnetic field induced by switching from $f_{m,2}$ (green line) to $f_{m,1}$ (black line). The red line shows a double exponential fit to the data. (c) Polarization times in dependence on the magnetic field strength. Lines are shown as guides to the eye. (d) Change of KR signal (black line) at $B = 5.62$ mT induced by switching from $f_{m,1} = 50$ kHz to $f_{m,2} = 1050$ kHz. The red line shows a measurement at the same conditions but with a dark time of 8 s. The dashed black line at the KR amplitude upon closing the shutter is shown as a guide to the eye. The inset shows the same signals, but over the full time range of about 8 s.

is switched from $f_{m,2} = 1050$ kHz to $f_{m,1} = 100$ kHz. The green line represents the KR signal at $f_{m,2} = 1050$ kHz. The black line shows the transient of the KR signal after switching to $f_{m,1} = 100$ kHz. By measuring the KR signal at a fixed magnetic field one detects the shift of the RSA peak from its position at $f_{m,2}$ to its position at $f_{m,1}$. The KR signal increases and saturates in less than a second. The rise of the KR signal is fitted with a double exponential function yielding rise times of $\tau_1 = 13 \pm 1$ ms and $\tau_2 = 136 \pm 1$ ms. We interpret these components as the minimal and maximal polarization time of the repolarization process with a stretched exponent. We tentatively assign the fastest polarization time to the strongly polarized nuclei near the center of the donors which are exposed to the strongest Knight field and are most sensitive to a change of the modulation frequency. On the other hand, the longest polarization time should result from the weaker polarized nuclei located farthest from the donors. These nuclei interact with a much weaker Knight field, so here the repolarization process occurs at a longer time scale.

Figure 1(c) shows these polarization times in dependence on the magnetic field. For these measurements $f_{m,1}$ is adjusted correspondingly to stay close to the optically induced NMR at higher fields. The red squares represent the minimal

polarization time (right axis), while the black circles show the maximal polarization time (left axis). Both components increase with magnetic field, which we tentatively assign to the increasing difference of the electron and the nuclear Zeeman splitting. We conclude that the time to polarize the nuclei is on the order of several tens of milliseconds (fastest) or several hundreds of milliseconds (longest) in the magnetic field range from 10 to 130 mT.

Note that all these measurements are conducted under illumination. A lower limit for the nuclear spin relaxation time in darkness without illumination T_1^{dark} can be estimated from the measurement shown in Fig. 1(d). Here the switching of f_m is combined with a shutter, which simultaneously blocks the pump and the probe beam. While the black line shows the continuous transient of the KR signal upon switching from $f_{m,1} = 50$ kHz to $f_{m,2} = 1050$ kHz modulation at $B = 5.62$ mT, the red line is measured with an additional dark time of 8 s. The shutter is closed at about 24 ms after the modulation frequency has been switched and reopened at about 8.006 s. Closing the shutter slows down the nuclear spin relaxation process, since it prevents a repolarization or depolarization due to spin flip-flops with spin polarized electrons [16]. The amplitudes of the KR signals before and after this dark time are nearly the same. Thus, we conclude that T_1^{dark} exceeds several tens of seconds.

Now we turn to measurements based on coherent manipulation of the nuclear spins with rf fields. The small peaks in the RSA spectrum at about $B = \pm 6.3$ mT, shown in Fig. 2(a), are caused by the NMR induced by helicity modulation of the pump with $f_m = 50$ kHz. In order to coherently control the nuclear spins one needs to determine the nuclear magnetic resonance frequency f_{NMR} at fixed external magnetic field. The inset shows an rf sweep with a peak-to-peak amplitude of 0.5 V ($A_{\text{rf}} = 0.5$ V_{pp}) to determine f_{NMR}. The measurement is performed at $B = 7.5$ mT (see arrow), where the KR signal is sensitive to the rf excitation of the nuclei. This rf excitation depolarizes the nuclei and thereby reduces the Overhauser field component along the external field ($B_N \parallel B$), if its frequency is at or close to f_{NMR} in the external magnetic field, so that the optically induced NMR vanishes and the KR signal exhibits a dip around f_{NMR}. The red line is a Lorentzian fit used to determine the NMR frequency $f_{\text{NMR}} = 60.93 \pm 0.01$ kHz.

We switch from this continuous-wave rf excitation to rf pulses of well-defined width to investigate the coherent properties of the nuclear spins. Figure 2(b) shows how the amplitude of the measured KR signal depends on the width of the rf pulses at resonant excitation of the NMR. We observe oscillations, which we interpret as Rabi oscillations, caused by the rotation of the nuclear spins around the effective magnetic field produced by the rf coil [17–19]. The red line is a fit with an exponentially damped oscillation which yields the Rabi frequency $f_R = 2.6$ kHz. This frequency can be used to calculate the effective induced magnetic field at a given rf voltage using the relation $B_{\text{eff}}[\text{mT}] = 0.1226[\text{mT/kHz}] f_R[\text{kHz}]$, where the gyromagnetic ratio γ for the ^{77}Se isotope $\gamma = 5.125\,385\,7 \times 10^7$ rad s^{-1} T^{-1} (see Ref. [20]) is used in $B_{\text{eff}} = 2\pi f_R/\gamma$. For the curve in Fig. 2(b) this yields $B_{\text{eff}} = 320$ μT. The inset of Fig. 2(b) shows the effective magnetic field in dependence on the rf amplitude. We obtain $B_{\text{eff}}[\mu\text{T}] = 79[\mu\text{T/V}_{\text{pp}}] A_{\text{rf}}[\text{V}_{\text{pp}}]$.

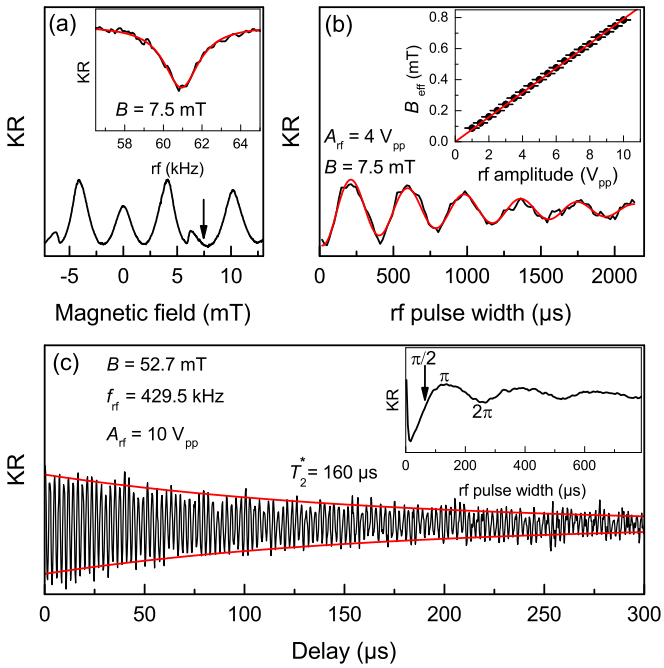

FIG. 2. (a) RSA spectrum measured at $f_m = 50$ kHz. The arrow shows the magnetic field position for the measurement of the KR signal in dependence on the applied rf fields. The inset shows the change of the KR signal induced by an rf field of 0.5 V_{pp}. (b) Rabi oscillations of ^{77}Se measured with 4 V_{pp} at $f_{\text{rf}} = 60.9$ kHz as a function of the rf pulse width. The inset shows the effective magnetic field of the rf coil in dependence on the rf voltage. (c) Ramsey fringes with a period of 2.33 μs. τ is the distance between the middle of the pulses (width about 65 μs) and the distance of 65 μs is subtracted. The fit with an exponentially damped oscillation is shown by its envelope (red line). The inset shows a Rabi oscillations measurement used to determine the length of a $\pi/2$ pulse.

The inset in Fig. 2(c) shows a Rabi oscillation measurement at $B = 52.7$ mT, $f_{\text{rf}} = 429.5$ kHz, and $A_{\text{rf}} = 10$ V_{pp}. It is used to determine the rf pulse width of a $\pi/2$ pulse. Using two $\pi/2$ pulses with a controllable delay τ between them allows one to measure Ramsey fringes and thereby determine the inhomogeneous spin dephasing time T_2^* of the nuclear spins [21–23]. Figure 2(c) demonstrates such a measurement. The first $\pi/2$ pulse creates a coherent superposition of the nuclear spins between the ground state $|0\rangle$ and the excited state $|1\rangle$ (both defined with respect to the constant external magnetic field) on the equator of the Bloch sphere [24]. The spins then precess in the equatorial plane, whereat the precession frequency is given by the Zeeman splitting of the nuclear spins. Due to this precession the nuclear spins acquire a relative phase with respect to the second $\pi/2$ pulse, so that this pulse will rotate the spins either to the $|0\rangle$ or the $|1\rangle$ state. The KR signal as a function of the delay τ, in turn, displays oscillations due to this periodic change between $|0\rangle$ and $|1\rangle$. The red line in Fig. 2(c) shows the envelope of a fit with an exponentially damped oscillation which yields $T_2^* = 160 \pm 5$ μs. At this time the nuclei run out of phase in their coherent precession.

To determine the nuclear spin coherence time T_2 one needs to apply an additional π pulse in between the two $\pi/2$ pulses

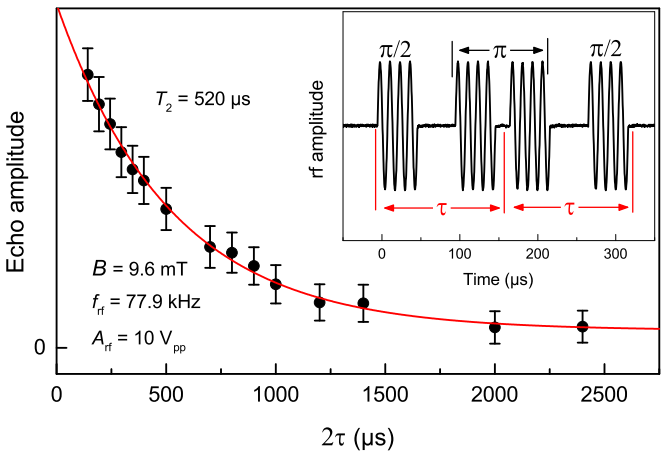

FIG. 3. Nuclear spin echo amplitude in dependence on the total time delay 2τ. The red line is an exponential fit. The inset illustrates the employed rf pulse scheme (time dependence of the normalized rf amplitude).

used for the Ramsey method. The π pulse applied after a time τ inverts the orientation of the spins which then rephase during the subsequent, second interval τ. This leads to a Hahn echo (nuclear spin echo) [25] at the time 2τ when the dephasing of the spins due to ensemble inhomogeneities is completely compensated due to inversion of the system at τ. The decay of the echo amplitude which is determined at approximately 2τ yields the T_2 time. Figure 3 demonstrates such a measurement at $B = 9.6$ mT and $A_{rf} = 10$ V_{pp}. The echo amplitude in dependence on the total time delay (2τ) between the $\pi/2$ pulses is best fitted with an exponential decay. This fit yields $T_2 = 520 \pm 25$ μs. The inset shows the used pulse sequence. The π pulse is constructed of two $\pi/2$ pulses of approximately 50 μs length (four cycles at $f_{rf} = 77.9$ kHz) in accordance with a Rabi oscillations measurement under the same conditions.

The evaluated times of the coherent nuclear spin dynamics in ZnSe:F under the conditions of the pump-probe experiment are in reasonable agreement with data for quantum dots, where the carriers are strongly localized. Our results for the spin dephasing time T_2^* and the spin coherence time T_2 have a similar order of magnitude as those reported for GaAs/(Al,Ga)As QWs [11] ($T_2^* = 90$ μs and $T_2 = 270$ μs and a single GaAs/(Al,Ga)As quantum dot [26] ($T_2^* = 16$ μs and $T_2 = 310$ μs). Note that in GaAs all nuclei have nonzero spin and the quadrupole interaction between the nuclei plays an important role in this system [27].

To summarize, we have demonstrated that the nuclear spin relaxation processes can be detected all-optically under the conditions of the TRKR experiment. We exploit the advantages of optical detection, such as high sensitivity and spectral selectivity [11]. We selectively study the spin dynamics of the nuclei in the vicinity of the fluorine donors, where a spatially inhomogeneous nuclear spin polarization is established under pulsed laser excitation. The detection by coherently precessing electrons instead of the polarization of the luminescence, as commonly used in measurements of the Hanle effect, allows one to select a single isotope, since one can work at higher magnetic fields, where the Larmor precession frequencies of different isotopes split up. Furthermore, the detection by coherently precessing electrons can be used to measure the effect of nuclear fields on an ensemble of electron spins, where one cannot resolve the Zeeman splitting in the nuclear Overhauser field [28] spectrally, e.g., as in the case of single dot spectroscopy [26,29,30].

We study the nuclear spin dynamics of the ^{77}Se isotope in fluorine-doped ZnSe under the same experimental conditions as in Ref. [9]. The fastest nuclear spin relaxation time T_1 or fastest polarization time under these conditions is found to be in the range from 6 to 90 ms at magnetic fields varied from 10 to 130 mT, while the longest polarization time is in the range from 100 to 430 ms. The nuclear spin coherence time is given by $T_2 = 520$ μs, so that the condition $T_1 \gg T_2$ is valid. Therefore, the spin temperature of the nuclei is established with the time T_2, which occurs much faster than the energy transfer to the lattice with the T_1 time. Thus, the nuclear spin polarization can be explained using the classical model of nuclear spin cooling. At this condition the nuclear spin temperature can be much lower than the lattice temperature.

We acknowledge the financial support by the Deutsche Forschungsgemeinschaft in the frame of the ICRC TRR 160, the Volkswagen Stiftung (Project No. 88360/90080), and the Russian Science Foundation (Grant No. 14-42-00015). T.K. acknowledges financial support of the Project SPANGL4Q of the Future and Emerging Technologies (FET) programme within the Seventh Framework Programme for Research of the European Commission, under FET-Open Grant No. FP7-284743. We thank V. L. Korenev for helpful discussions.

[1] K. Sanaka, A. Pawlis, T. D. Ladd, K. Lischka, and Y. Yamamoto, Phys. Rev. Lett. **103**, 053601 (2009).

[2] K. Sanaka, A. Pawlis, T. D. Ladd, D. J. Sleiter, K. Lischka, and Y. Yamamoto, Nano Lett. **12**, 4611 (2012).

[3] K. De Greve, S. M. Clark, D. Sleiter, K. Sanaka, T. D. Ladd, M. Panfilova, A. Pawlis, K. Lischka, and Y. Yamamoto, Appl. Phys. Lett. **97** 241913 (2010).

[4] Y. M. Kim, D. Sleiter, K. Sanaka, Y. Yamamoto, J. Meijer, K. Lischka, and A. Pawlis, Phys. Rev. B **85**, 085302 (2012).

[5] D. J. Sleiter, K. Sanaka, Y. M. Kim, K. Lischka, A. Pawlis, and Y. Yamamoto, Nano Lett. **13**, 116 (2013).

[6] A. Greilich, A. Pawlis, F. Liu, O. A. Yugov, D. R. Yakovlev, K. Lischka, Y. Yamamoto, and M. Bayer, Phys. Rev. B **85**, 121303 (2012).

[7] F. Heisterkamp, E. A. Zhukov, A. Greilich, D. R. Yakovlev, V. L. Korenev, A. Pawlis, and M. Bayer, Phys. Rev. B **91**, 235432 (2015).

[8] A. Greilich, A. Shabaev, D. R. Yakovlev, A. L. Efros, I. A. Yugova, D. Reuter, A. D. Wieck, and M. Bayer, Science **317**, 1896 (2007).

[9] F. Heisterkamp, A. Greilich, E. A. Zhukov, E. Kirstein, T. Kazimierczuk, V. L. Korenev, I. A. Yugova, D. R. Yakovlev, A. Pawlis, and M. Bayer, Phys. Rev. B **92**, 245441 (2015).

[10] V. G. Fleisher and I. A. Merkulov, in *Optical Orientation*, edited by F. Meier and B. Zakharchenya, Modern Problems in Condensed Matter Sciences (North-Holland, Amsterdam, 1984), Chap. 5.

[11] H. Sanada, Y. Kondo, S. Matsuzaka, K. Morita, C. Y. Hu, Y. Ohno, and H. Ohno, Phys. Rev. Lett. **96**, 067602 (2006).

[12] Y. Kondo, M. Ono, S. Matsuzaka, K. Morita, H. Sanada, Y. Ohno, and H. Ohno, Phys. Rev. Lett. **101**, 207601 (2008).

[13] E. A. Zhukov, A. Greilich, D. R. Yakovlev, K. V. Kavokin, I. A. Yugova, O. A. Yugov, D. Suter, G. Karczewski, T. Wojtowicz, J. Kossut, V. V. Petrov, Y. K. Dolgikh, A. Pawlis, and M. Bayer, Phys. Rev. B **90**, 085311 (2014).

[14] J. M. Kikkawa and D. D. Awschalom, Phys. Rev. Lett. **80**, 4313 (1998).

[15] I. A. Yugova, M. M. Glazov, D. R. Yakovlev, A. A. Sokolova, and M. Bayer, Phys. Rev. B **85**, 125304 (2012).

[16] V. L. Korenev, Phys. Rev. Lett. **99**, 256405 (2007).

[17] I. I. Rabi, Phys. Rev. **51**, 652 (1937).

[18] I. I. Rabi, J. R. Zacharias, S. Millman, and P. Kusch, Phys. Rev. **53**, 318 (1938).

[19] I. I. Rabi, S. Millman, P. Kusch, and J. R. Zacharias, Phys. Rev. **55**, 526 (1939).

[20] R. K. Harris, E. D. Becker, S. M. Cabral De Menezes, R. Goodfellow, and P. Granger, Concept. Magnetic Res. **14**, 326 (2002).

[21] N. F. Ramsey, Phys. Rev. **76**, 996 (1949).

[22] N. F. Ramsey, Phys. Rev. **78**, 695 (1950).

[23] N. Ramsey, Appl. Phys. B **60**, 85 (1995).

[24] F. Bloch, Phys. Rev. **70**, 460 (1946).

[25] E. L. Hahn, Phys. Rev. **80**, 580 (1950).

[26] M. N. Makhonin, K. V. Kavokin, P. Senellart, A. Lemaître, A. J. Ramsay, M. S. Skolnick, and A. I. Tartakovskii, Nat. Mater. **10**, 844 (2011).

[27] E. A. Chekhovich, M. Hopkinson, M. S. Skolnick, and A. I. Tartakovskii, Nat. Commun. **6**, 1 (2014).

[28] A. W. Overhauser, Phys. Rev. **92**, 411 (1953).

[29] E. A. Chekhovich, M. N. Makhonin, A. I. Tartakovskii, A. Yacoby, H. Bluhm, K. C. Nowack, and L. M. K. Vandersypen, Nat. Mater. **12**, 494 (2013).

[30] E. A. Chekhovich, M. M. Glazov, A. B. Krysa, M. Hopkinson, P. Senellart, A. Lemaître, M. S. Skolnick, and A. I. Tartakovskii, Nat. Phys. **9**, 74 (2013).